Adsorption of aluminum from aqueous solutions utilizing waste polyethylene terephthalate derived activated carbon

Yu Shuang Ren[a], Muhammad Ilyas[b,c], Muhammad Yasir[d,*], Sami Ur Rahman[e]

[a]*School of Economics and Management, Jilin Jianzhu University, Chang Chun 130117, China, email: rysmiracle@126.com (Y.S. Ren)*
[b]*Department of Environmental Sciences, University of Peshawar, Peshawar, Khyber Pakhtunkhwa, Pakistan, email: sirfilyas@yahoo.com (M. Ilyas)*
[c]*Department of Environmental Sciences, Shaheed Benazir Bhutto University Wari Campus, Dir Upper, Khyber Pakhtunkhwa, Pakistan*
[d]*College of Oceanography and Space Informatics, China University of Petroleum (East China), Qingdao 266580, China, Tel.: +8615621473689; email: ls1801004@s.upc.edu.cn (M. Yasir)*
[e]*College of Environmental Science and Engineering, Fujian Normal University, Fuzhou 50007, PR China, email: samisirhindi@gmail.com (S. Ur Rahman)*

ABSTRACT

This study aims to adsorb aluminum (Al^{3+}) from aqueous solutions through batch experiments utilizing activated carbon (AC). Waste polyethylene terephthalate was carbonized in a N_2 environment and then chemically activated with 1 M KOH to produce AC. Fourier-transform infrared spectroscopy, surface area analysis, as well as scanning electron microscopy were used to analyze the AC. The pertinent adsorption behaviors of AC for Al^{3+} have been studied, including adsorption isotherms, adsorption kinetics, the effect of initial Al^{3+} concentration, adsorbent dosage, contact time, as well as pH, etc. According to the results, AC has the maximum ability for adsorbing Al^{3+} from aqueous solution (>95%). The findings show that the pseudo-second-order equation can accurately predict the adsorption kinetics of AC for Al^{3+}, and that the experimental data and Langmuir isotherm model match well, demonstrating homogeneous monolayer adsorption. According to the research findings, AC may be used as a sort of very effective adsorbent in the treatment of wastewater, which would enable a simple approach for the removal of Al^{3+}.

Keywords: Activated carbon; Aqueous solution; Adsorptive removal; Aluminum

1. Introduction

After oxygen and silicon, aluminium (Al^{3+}) is the third most common element in the Earth's crust. It is a poisonous metal that is not required for human life [1]. Al^{3+} is also contained in the deposited particulate matter [2]. The excessive use of aluminum salts (alum) in chemical treatment processes in water treatment plants as a coagulant to remove organic matter, microorganisms, color, as well as turbidity [3,4]. Al^{3+} can cause neurological disorders, including Parkinson's Dementia, amyotrophic lateral sclerosis, and Alzheimer's disease (AD) [5,6]. The World Health Organization estimates that the number of people infected with the AD disease will reach 9 million by 2030 [1].

Much effort has been done on wastewater treatment during the last few years [7]. Diverse methods are created to cater the elimination of toxic elements as of wastewater, which incorporate membrane inlet mass spectrometry method [8], aerobic granule in continuous-flow [9] reduction, chemical precipitation, chemical reduction/oxidation, electrochemical treatment, photocatalytic reduction, membrane separation, ion exchange, coagulation or flocculation,

* Corresponding author.

chemical precipitation, complexation, filtrations, electrochemical precipitation, solid phase adsorption, biosorption, adsorption [10–24], biological denitrification treatment [25], photoinduced reaction [26], direct hydration reaction [27]. The majority of these approaches, however, are hindered by issues like expensive startup and maintenance costs and unclear working mechanisms [28].

Adsorption is an important wastewater treatment technique that is widely used to remove toxic metals from wastewater [29–37]. Assortment of adsorbents utilized for this reason incorporates chemically treated biosorbents [38,39], novel coagulant [40], Fe-doped and terephthalaldehyde-modified carbon nitride [41], RuPt/AC bimetallic catalysts [42], polyacrylonitrile/Na-Y-zeolite composite [43], biochar/bentonite/waste polyethylene terephthalate as well as biochar/bentonite/waste polystyrene [29], *Phoenix dactylifera* coir wastes [44], magnetic chitosan grafted with Schiff's base polymer [45], L-cystein-modified montmorillonite-immobilized alginate nanocomposite [46], microalgae [47], synthetic chelating resin [48], poly(methyl methacrylate)-grafted alginate/Fe_3O_4 nanocomposite [49], various other adsorbents [50], biosorbents [51], montmorillonite clay [52], ligand embedded nano-conjugate adsorbent [53], greenly synthesized nanoengineered materials [54], bamboo charcoal [55], nanocomposites [56], non-thermal plasma catalysis [57], green synthesis of silver nanoparticles [58], ligand based composite material [59], metal/mineral-incorporating materials [60], iron oxide-impregnated dextrin nanocomposite [61], ether based mesoporous adsorbent [62], magnetic glycine-modified chitosan [63], papaya peel carbon [64], ligand functionalized organic–inorganic based novel composite [65], thiourea-formaldehyde resin and its magnetic derivative [66], thin-film composite nanofiltration membrane [67], phthalide-derived analogues [68], dimeric salophen platinum(II) complexes [69], chitosan grafted polyaniline [70], modified conjugate material [71], CuO and $Cu(OH)_2$ embedded chitosan [72], waste rubber tires [73], ligand doped conjugate adsorbent [74], magnetic glycidyl methacrylate resin [75], iron based metal organic framework [76], nano zero-valent iron [77], natural wood-derived charcoal embedded with bimetallic iron/cobalt sites [78], element sulfur-based autotrophic denitrification constructed wetland [79], novel optical adsorbent [80], ligand based efficient conjugate anomaterials [81], novel facial composite adsorbent [82,83], nanoadsorbent [84], MoS_2/Fe_3O_4/aminosilane/glycidyl methacrylate/melamine dendrimer grafted polystyrene/poly(N-vinylcaprolactam) nanocomposite [85], 3D polymer nanomagnetic ($3D/GO/Fe_3O_4$) [86], and graphene oxide modified with 4-aminodiphenylamine [87].

Over the past 50 y, plastic usage has dramatically increased over the world. The growing manufacturing and use of plastic is threatening the environment because of its improper dumping and waste management. A variety of methods are offered for dealing with expanding plastic solid waste, including land filling, incineration, recycling, and its conversion into liquid or gaseous fuels [29]. After being evaluated critically, each of these methods has been found to have certain drawbacks. However, using plastic wastes in carbonized form as adsorbents to remove various hazardous chemicals from wastewater is a more feasible and environmentally beneficial method of reducing water

pollution. In this study, activated carbon (AC) has been successfully prepared by a simple and low-cost method. The structural characteristics of AC and the adsorption state of Al^{3+} were studied. Through batch studies, the effectiveness of AC adsorption was evaluated and its adsorption behavior on Al^{3+} was carefully examined, including the effects of initial Al^{3+} concentration, temperature, contact time, pH, adsorbent dosage, adsorption isotherm, and adsorption kinetics. This study makes a significant contribution to the removal of Al^{3+} from wastewater and establishes a new benchmark for reducing environmental pollution by reducing solid waste. This in turn enhances the aesthetic value of the local environment.

2. Material and methods

2.1. Sample collection and preparation

Samples of waste polyethylene terephthalate (wPET) were collected from the municipal solid wastes. After being cleansed with distilled water, the wPET samples were allowed to dry at room temperature before being shredded into tiny flakes. The water that was used in this study was deionized, and all chemicals and reagents were of analytical grade and used without additional purification. Stock solutions of Al^{3+} (1,000 mg/L) were prepared by dissolving its salt aluminium nitrate $(Al(NO_3)_3)$ in 1,000 mL of deionized water, and the experimental solutions of the desired concentration were prepared by diluting the stock solution with deionized water.

2.2. Synthesis and characterization of activated carbon

Samples of wPET were collected from the street waste bins. The wPET samples were washed, dried, and shredded to small pieces. The waste plastic samples were converted into AC by carbonization in a specially designed steel reactor under inert atmosphere at high temperature. The steel reactor containing 5 g of wPET was placed in the tube furnace, linked to the nitrogen supply, and heated for 1 h at 600°C as indicated in Fig. 1. The AC was removed from the reactor and chemically activated by treating it alternately with 1 M KOH in accordance with the method described in the literature [83,88]. The solid carbon was finally ground to fine powder and passed through a sieve with pore size 250 μm and then stored in glass vials for further study.

Scanning electron microscopy (SEM), Fourier-transform infrared spectroscopy (FTIR), and surface area were used to characterize the AC that was synthesized in the laboratory. Using a scanning electron microscope made by JEOL (Tokyo, Japan), the surface morphology of the AC was investigated. A Nicolet iS10 FTIR spectrometer (Cary 630, Agilent Technologies, USA) with a scanning range of 4,000–400 cm^{-1} was used to measure the FTIR spectra. The average pore size, total pore volume, and specific surface area were calculated using a Quantachrome, USA, model NOVA 2200e porosimetry system and surface area.

2.3. Al^{3+} adsorption measurements of AC

Adsorption of Al^{3+} from aqueous solution over AC was studied in batch mode adsorption experiments. About
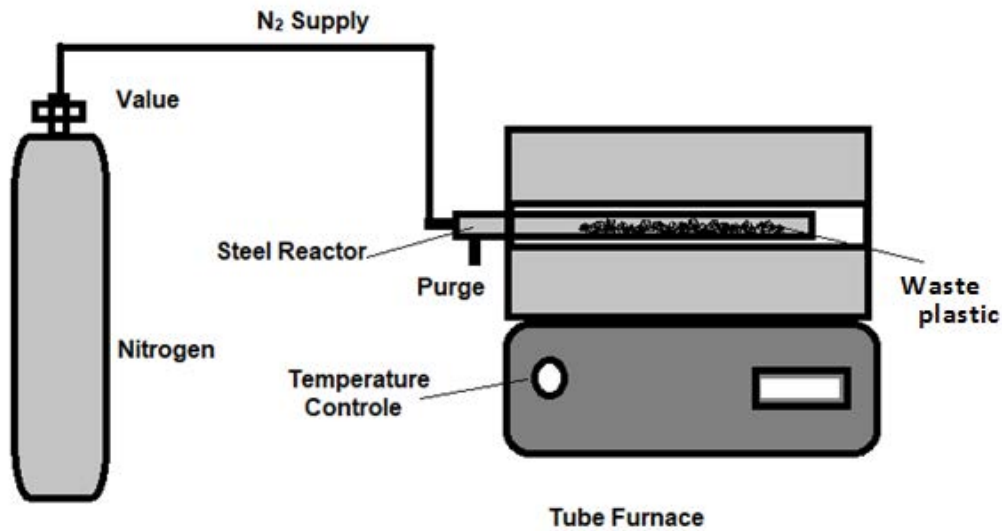
Fig. 1. Diagrammatic presentation of activated carbon in the lab.

100 mL of aqueous solution containing Al^{3+} was taken in 500 mL Erlenmeyer flasks at 24°C ± 2°C, a definite amount of AC adsorbent were added to it and stirred on a magnetic stirrer with 150 rpm speed until equilibrium was reached. Several variables were measured in the study, including dosage of AC (0.05, 0.10, 0.15, and 0.20 g), contact time (15, 30, 45, 60, and 90 min), Al^{3+} concentrations (10, 20, and 30 mg/L) and pH of solutions (1–7), pH was adjusted by adding 0.1 M NaOH to the solution as required.

Atomic absorption spectrophotometer (AAnalyst 700, PerkinElmer, USA), operating in flame mode, was used to quantify the amount of Al^{3+} [89]. Calculations of the corresponding removal percentage (%) and adsorption capacity (q_e) of AC (mg/g) were made using Eqs. (1) and (2), respectively [29,89].

$$\%MR = \frac{(C_o - C_i)}{C_o} \times 100 \tag{1}$$

where C_i and C_o represent the final and initial concentration (mg/L).

$$q_e = \frac{\left[(C_o - C_i) \times V\right]}{m} \tag{2}$$

where V is the volume (L) of the stock solution and m is the adsorbent weight (g). For all tests carried out, the mean values only of triplicate were presented.

To assess the fitness of the isotherm, as well as the kinetic equations to the experimental data, the root mean square error (RMSE) was utilized to determine the isotherm along with kinetic constants. RMSE can be defined as:

$$RMSE = \sqrt{\frac{1}{N-2} \sum_{i=1}^{N} \left(q_{e,\exp} - q_{e,\text{calc}}\right)^2} \tag{3}$$

where N is the number of observations and the subscripts "calc" and "exp" show the calculated and experimental values in the experimental data. The small the RMSE value, the better the curve fitting [90].

Adsorption kinetics was investigated by applying different rate equations [91–93]. Construction of linear plots was studied by applying pseudo-first and pseudo-second-order kinetic models. The pseudo-first-order rate constant was calculated using the following Eq. (4) [29,89]:

$$\ln\left(q_e - q_t\right) = \ln q_e + k_1 t \tag{4}$$

The pseudo-second-order rate constant was determined using following equation [29,89]:

$$\frac{t}{q_t} = \frac{t}{q_e} + \frac{1}{K_2 q_e^2} \tag{5}$$

Different adsorption isotherms were also applied to investigate the nature of adsorption. The Langmuir isotherm equation was used in the following form [29,89]:

$$\frac{C_e}{q_e} = \frac{1}{K Q_{\max}} + \frac{C_e}{Q_{\max}} \tag{6}$$

The Freundlich adsorption isotherm was applied as the following equation [29,89]:

$$\ln q_e = \ln K_f + \frac{1}{n} \ln C_e \tag{7}$$

where q_e represents the concentration adsorbed on the composite (mg/g), C_e is the equilibrium concentration of Al^{3+} (mg/L), while the constant and the adsorption coefficient are represented by n and K_f for the model, respectively.

3. Results and discussion

3.1. Characterization of AC

Specific surface area analysis, SEM, and FTIR were used to depict AC. SEM observations of the AC are shown

in Fig. 2a and b, where it is clear that the surface of AC is relatively rough and porous, and it is made up of KOH particles, many of which have micropores that could serve as additional Al^{3+} adsorption sites (Fig. 2a). After adsorbing Al^{3+}, the surface of AC appeared glossy, smooth, and had a closed pore structure, as shown in Fig. 2b. This change may be the result of physicochemical interactions between the functional groups on the surface of AC and Al^{3+}.

Fig. 3a and b show FTIR spectra of wPET and AC. The characteristic infrared absorption bands of wPET (Fig. 3a) at 691 cm^{-1} (C–H, stretching), 722 cm^{-1} (C–H, stretch), 1,009 cm^{-1} (C–O–C, stretching), 1,100 cm^{-1} (C–O, stretching vibration), 1,240 cm^{-1} (C=C, stretch), 1,409 cm^{-1} (CH_2 stretching), 1,594 cm^{-1} (C=C, stretching), and 1,696 cm^{-1} (C=O, stretch) are clearly observed [34]. The FTIR spectrum of AC (Fig. 3b) showed that the AC had functional groups of wPET. The noticeable absorption peaks at 722 cm^{-1} (C–H, stretch), 779 cm^{-1} (C–H, stretch), 872 cm^{-1} (C–H, stretch), 1,017 cm^{-1} (C–O–C, stretching), 1,100 cm^{-1} (C–O, stretching vibration), 1,250 cm^{-1} (C=C, stretch), 1,406 cm^{-1} (CH_2, stretching), and 1,681 cm^{-1} (C=O, stretch) [94]. These results suggest that wPET-derived AC contains various oxy-functional groups that may be due to surface oxidation of AC. The point of zero charge (PZC) was found to be 4.25 (Fig. 4), and its surface will be negatively and positively charged at pH values above and below the PZC.

Surface properties such as total pore volume (V_t), mean pore radius (R_p), Brunauer–Emmett–Teller (BET) surface area (S_{BET}), and Barrett–Joyner–Halenda (BJH) surface area (S_{BJH}) were calculated for AC. Results show that wPET-AC exhibits S_{BET} of 65.35 m^2/g, S_{BJH} of 11.02 m^2/g, V_t of 0.009 cm^3/g and an R_p of 15.02 Å. After adsorption, the surface properties are S_{BET} 2.40 m^2/g, S_{BJH} 1.95 m^2/g, V_t 0.0001 cm^3/g and R_P 2.90 Å. The surface properties decreased after adsorption, confirming the adsorption of Al^{3+}.

3.2. Effect of process parameters

We evaluated the adsorption under various conditions of pH, Al^{3+} concentration, adsorbent dosage, and contact time in order to determine the optimal conditions necessary for maximum Al^{3+} adsorption.

3.2.1. Effect of contact time

The tests were conducted at various adsorption times, that is, 15, 30, 45, 60, and 90 min, to determine the effect of adsorption time on the percentage adsorption of Al^{3+} on the AC. The results are displayed in Fig. 5, which demonstrates that the adsorption of Al^{3+} increases linearly with an increase in adsorption duration and reaches its maximum within 90 min. However, an increase in adsorption
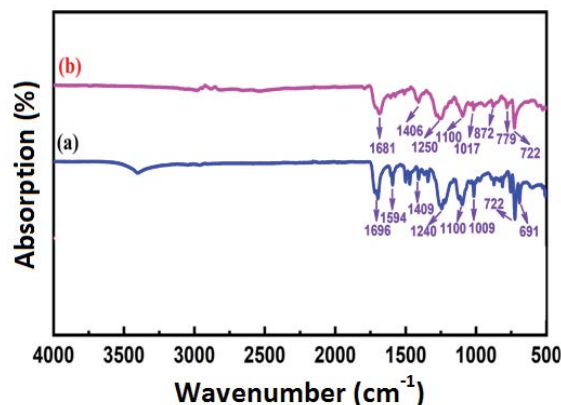
Fig. 3. Fourier-transform infrared spectra of (a) waste polyethylene terephthalate and (b) activated carbon.
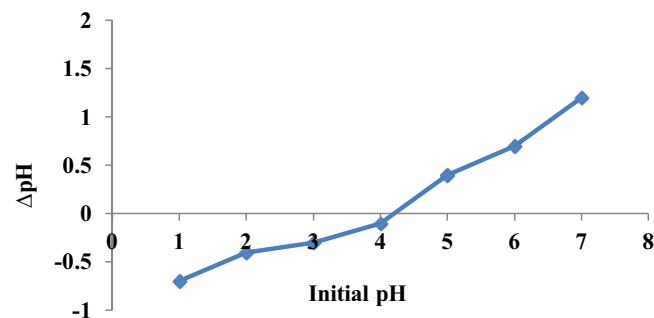
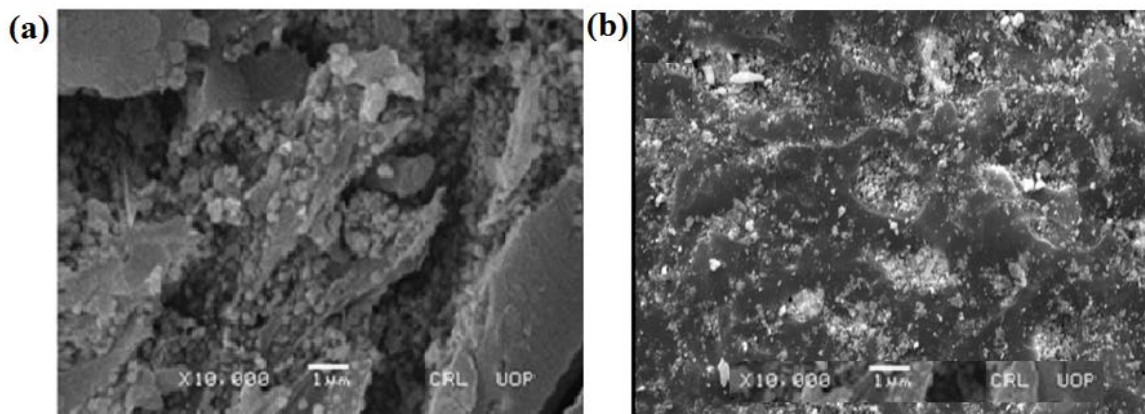Fig. 4. Determination of point of zero charge of activated carbon.

Fig. 2. Scanning electron microscopy images of activated carbon before Al^{3+} adsorption (a), and activated carbon after Al^{3+} adsorption (b).

beyond this point has no further effect on adsorption. These results suggest that the adsorption rate initially increases with the number of accessible adsorption sites on the AC surface as the adsorption time increases. The voids were filled within 90 min, and thereafter, the adsorption became steady [29,88,89,94]. These findings led to the decision that 90 min was the ideal adsorption time.

3.2.2. Effect of initial Al^{3+} concentration

At various initial Al^{3+} concentrations, the adsorption of Al^{3+} by AC was studied. Fig. 6 displays the data. This implies that the rate of Al^{3+} adsorption on AC increases as the initial Al^{3+} concentration rises from 10 to 30 mg/L. This results from Al^{3+} adhering to the surface-active sites of AC when the initial Al^{3+} concentration is increased. As Al^{3+} concentration rises, the existence of a large concentration gradient produces a more grounded primary impetus that uses active sites to enhance the amount of AC that can be absorbed per unit mass while overcoming mass exchange resistance [29]. Three removal mechanisms, chelation, ion exchange, and electrostatic attraction mechanism existed simultaneously when the AC was used [28,94–96].

3.2.3. Effect of AC adsorbent dosage

The amount of adsorbent used also has a big impact on how much toxic metal is absorbed. The ability of the adsorbent to be used efficiently while maintaining high adsorption effectiveness is typically necessary for the investigation of the optimal adsorbent dosage. The necessary adsorbent dosage was adjusted between 0.05 and 0.20 g/L in order to find the ideal value for Al^{3+} adsorption on AC. The adsorption effect of AC adsorbent dose from an aqueous medium is depicted in Fig. 7. As can be shown in Fig. 7, the adsorption capacity of the adsorbent for Al^{3+} decreases as the adsorption rate rises. This can be attributed to Al^{3+} competitive adsorption tendency to disperse across the wide surface of the adsorbent, which lowers the adsorption capacity per unit mass of AC [98]. The removal rate is almost high when the adsorbent dosage is 0.20 g/L. Accordingly, 0.20 g/L of AC would be utilised as the ideal adsorbent dosage in the upcoming studies based on the aforementioned experimental findings in order to thoroughly examine its adsorption ability.

3.2.4. Effect of pH

Investigating the ideal pH for Al^{3+} adsorption is crucial because the pH of the investigated solution system is crucial for both the state of the adsorbate and the surface chemical characteristics of the adsorbent. It has been studied how well AC adsorbs Al^{3+} in the pH range of 2–6. The related adsorption tests were carried out at 25°C and a pH range of 1–7 in order to assess the impact of pH on the adsorption of Al^{3+} on AC and to optimize a specific pH for maximum adsorption efficiency. Fig. 8 displays the final result. Fig. 8 clearly illustrates how the variation trends are similar in nature and how the adsorption capacity quickly rises with increasing pH. The results showed that the adsorption process was highly dependent on pH, and
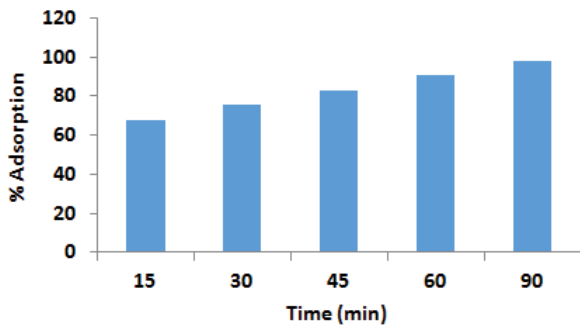
Fig. 5. Effect of contact time (15, 30, 45, 60, and 90 min) on % adsorption of Al^{3+} over activated carbon.
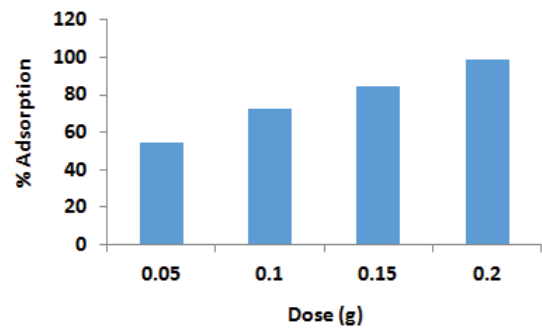
Fig. 7. Effect of dose (0.05, 0.10, 0.15, and 0.20 g) on % adsorption of Al^{3+} over activated carbon.
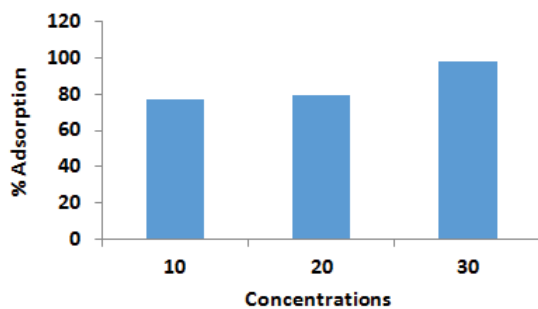
Fig. 6. Effect of concentrations (10, 20, and 30 mg/L) on % adsorption of Al^{3+} over activated carbon.
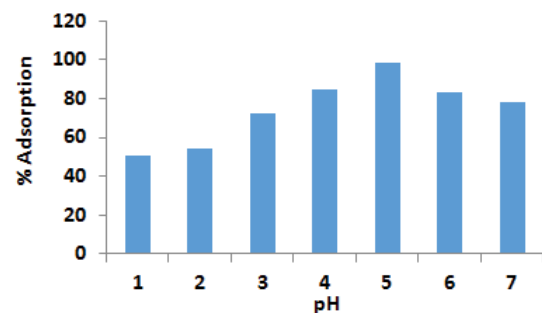
Fig. 8. Effect of pH (2, 3, 4, 5, 6, and 7) on % adsorption of Al^{3+} over activated carbon.

increasing the pH from 1 to 5 increased the adsorption of Al^{3+}. However, adsorption decreased if the pH value was increased, so pH 5 was chosen for further study. The PZC value of AC is 4.25, indicating that its surface is positively and negatively charged at pH values below and above the PZC, respectively. The data showed that there was no significant difference in the adsorption of Al^{3+} in the pH range of 1–4, which may be because there are too many H^+ ions competing with Al^{3+} for the same adsorption sites [29,94]. Therefore, the subsequent Al^{3+} adsorption experiments are conducted in the solution condition of pH = 5.0.

3.3. Adsorption kinetics

The kinetic data are crucial for choosing the best conditions while developing the AC adsorption system. Two well-known kinetic models, pseudo-first-order and pseudo-second-order equations, were applied to the data for this purpose. According to Table 1, the obtained coefficient of the pseudo-second-order model was high for the AC, indicating that this model had greater conformance than the pseudo-first-order model at describing the adsorption behavior of AC for Al^{3+}. The adsorption kinetics are thus better described by the pseudo-second-order model, which also suggests that chemisorption mostly governs the adsorption of Al^{3+} over AC.

3.4. Isotherm study

We can determine how the adsorbates are distributed between the solution and the adsorbent when the adsorption process is at an equilibrium state by studying the adsorption isotherms [99], which is essential and required to comprehend the interactions between the adsorbate and adsorbent and to establish an appropriate correlation of adsorption equilibria in order to optimize the adsorption

Table 1
Kinetic parameters of Al^{3+} adsorption over activated carbon

Pseudo-first-order equation parameters		Pseudo-second-order equation parameters	
K_1 (min^{-1})	0.039	K_2 (mg/g·min)	0.001
q_e (mg/g)	2.254	q_e (mg/g)	0.192
R^2	0.960	R^2	0.986
RMSE	0.460	RMSE	0.090

Table 2
Al^{3+} adsorption isotherm parameters with their corresponding correlation coefficients

Langmuir isotherm parameters		Freundlich isotherm parameters	
	Al^{3+}		Al^{3+}
q_m (mg/g)	0.141	N	1.832
K_1	0.673	K_f	2.639
R^2	0.989	R^2	0.976
RMSE	0.053	RMSE	0.250

system. The fitting of the suitable model to the isotherm data analysis can be employed in the design process. Studies on the relevant adsorption isotherms have been done in order to examine the link between equilibrium adsorption capacity and equilibrium concentration for the AC. Table 2 provides a summary of the derived isotherm constants and correlation coefficients (R^2) for Freundlich and Langmuir isotherms as well as their corresponding RMSE values. The Langmuir isotherm model is predicated on the idea that a surface monolayer will only be able to adsorb homogenous substances at a few number of adsorption sites.

3.5. Industrial wastewater treatment

Due to the widespread industrialization and rapid population growth around the world, the management of industrial and municipal wastewater has become an inevitable challenge in today's world [29]. Excessive urbanization has caused serious environmental pollution, which is related to the high consumption of products containing trace metals and heavy metals in different concentrations produced by factories [88,90]. A variety of harmful metals enters water bodies and enters the food chain, causing serious health risks to humans. Different toxic metals have been reported to cause different physiological toxicity, but in general, trace metals and heavy metals are known to be associated with damage to nerves, kidneys, liver, bones, and block enzyme functional groups [29]. Since toxic metal ions persist in wastewater, removal of toxic metal ions is critical. Toxic metals can be removed and recovered from our environment and wastewater using a variety of physical and chemical techniques. The removal of Al^{3+} from wastewater by AC adsorbent was studied by batch adsorption test. The experimental results show that under the optimal conditions (concentration 30 mg/L, adsorbent dosage 0.20 g, contact time 90 min, temperature 60°C, pH 5), the maximum adsorption rate of AC to Al^{3+} is 98.44%.

3.6. Comparison of adsorption potential of different adsorbents

The comparative adsorption efficiencies of the adsorbents, specifically AC and different adsorption media, are compiled in Table 3 for Al^{3+} adsorption. The statistics demonstrate that AC has higher adsorption efficiency than any other adsorbents. The greater surface area of AC, which is what led to the higher adsorption capacity employed in our investigation, seems to be responsible for the efficiency of AC.

3.7. Desorption experiment

Desorption/regeneration of adsorbents is one of the key components of metal removal processes since it regulates the cost of water treatment technology [88,94]. In various experiments, adsorbents were recovered and effectively regenerated using salts (such as NH_4NO_3, $CaCl_2$-$2H_2O$, KNO_3, $(NH_4)_2SO_4$, $C_6H_5Na_3O_7$-$2H_2O$, KNO_3, NaCl and KCl), buffer solutions (such as bicarbonate and phosphate), acids (such as H_2SO_4, HCOOH, HCl, CH_3COOH, and HNO_3), chelating agents as well as deionized water [88,89,94]. In this study, deionized water and 0.1 M HCl were used for

Table 3
Comparison of different adsorbents used for Al^{3+} adsorption

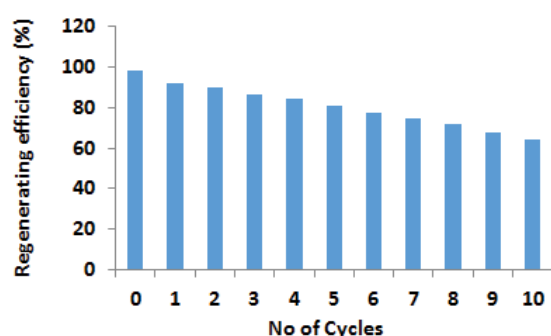| Adsorbent	Adsorption potential (mg/g) Al^{3+}	References
Activated carbon	137.70	This article
PAN beads as-prepared	0.25	[100]
BDH activated carbon	0.02	[101]
Date pit	0.31	[101]
AXAD-16 resin	24.30	[102]
201 × 8 anion resin	5.60	[103]
XAD-4	4.40	[104]
IIP-PEI/SiO$_2$	53.50	[105]

Fig. 9. Regenerating efficiency of activated carbon.

desorption experiments. The spent AC was added to 0.1 M HCl and stirred for 30 min, then the AC was recovered by filtration and subsequently dried in an oven. The dry, clean AC is then used to absorb a new batch of wastewater (Fig. 9).

4. Conclusion

Herein, we have provided a simple method for preparing AC from wPET. The developed AC can be severed as an efficient adsorbent to remove Al^{3+} from aqueous solution as well as wastewater (>95%). The effective synthesis and microstructure of the AC were confirmed by a number of characterization techniques. AC possess a porous structure and large specific surface area, which provides sufficient active adsorption sites for Al^{3+}. Moreover, the external factors affecting the adsorption performance were fully investigated. The outcomes demonstrated the AC superior reusability and high removal efficiency. The adsorption process is well modelled by the pseudo-second-order (R^2 = 0.986) and Langmuir models (R^2 = 0.989). The findings of this work suggest that AC is a potential adsorbent with the potential to effectively remove Al^{3+} from aqueous solutions. For future work, we plan to examine the adsorption efficiency of AC for organic and inorganic pollutants.

Research funding

Conflict of interest

Authors state no conflict of interest.

Informed consent

Informed consent is not applicable.

Ethical approval

The conducted research is not related to either human or animal use.

References

[1] D. Diaconu, M.M. Nănău, E. Nechifor, O. Nechifor, R. Diaconu, Aluminum concentration in drinking water from Moldova territory, Romania, Ovidius Univ. Ann. Chem., 20 (2009) 115–118.

[2] R.F. Fard, K. Naddafi, M.S. Hassanvand, M. Khazaei, F. Rahmani, Trends of metals enrichment in deposited particulate matter at semi-arid area of Iran, Environ. Sci. Pollut. Res., 25 (2018) 18737–18751.

[3] M.S. Qaiyum, M.S. Shaharudin, A.I. Syazwan, A. Muhaimin, Health risk assessment after exposure to aluminium in drinking water between two different villages, J. Water Resour. Prot., 3 (2011) 268–274.

[4] M.R. Siti Farizwana, S. Mazrura, A. Zurahanim Fasha, G. Ahmad Rohi, Determination of aluminium and physicochemical parameters in the palm oil estates water supply at Johor, Malaysia, J. Environ. Public Health, 2010 (2010) 615176, doi: 10.1155/2010/615176.

[5] L. Simonsen, H. Johnsen, S.P. Lund, E. Matikainen, U. Midtgård, A. Wennberg, Evaluation of neurotoxicity data: a methodological approach to classification of neurotoxic chemicals, Scand. J. Work Environ. Health., 20 (1994) 1–2.

[6] M. Gidding, Aluminum, Environmental and Workplace Health Canadian Drinking Water Quality, Canada, 1998.

[7] Z. Guo, R. Zhan, Y. Shi, D. Zhu, J. Pan, C. Yang, Y. Wang, J. Wang, Innovative and green utilization of zinc-bearing dust by hydrogen reduction: recovery of zinc and lead, and synergetic preparation of Fe/C micro-electrolysis materials, Chem. Eng. J., 456 (2023) 141157, doi: 10.1016/j.cej.2022.141157.

[8] X. Lin, K. Lu, A.K. Hardison, Z. Liu, X. Xu, D. Gao, J. Gong, W.S. Gardner. Membrane inlet mass spectrometry method (REOX/MIMS) to measure ^{15}N-nitrate in isotope-enrichment experiments, Ecol. Indic., 126 (2021) 107639, doi: 10.1016/j.ecolind.2021.107639.

[9] D. Xu, J. Li, J. Liu, X. Qu, H. Ma, Advances in continuous flow aerobic granular sludge: a review, Process Saf. Environ. Prot., 163 (2022) 27–35.

[10] R. Camarillo, Á. Pérez, P. Cañizares, A. de Lucas, Removal of heavy metal ions by polymer enhanced ultrafiltration: batch process modeling and thermodynamics of complexation reactions, Desalination, 286 (2012) 193–199.

[11] R. Aravindhan, B. Madhan, J.R. Rao, B.U. Nair, T. Ramasami, Bioaccumulation of chromium from tannery wastewater: an approach for chrome recovery and reuse, Environ. Sci. Technol., 38 (2004) 300–306.

[12] J.J. Testa, M.A. Grela, M.I. Litter, Heterogeneous photo-catalytic reduction of chromium(VI) over TiO$_2$ particles in the presence of oxalate: involvement of Cr(V) species, Environ. Sci. Technol., 38 (2004) 1589–1594.

[13] C.A. Kozlowski, W. Walkowiak, Removal of chromium(VI) from aqueous solutions by polymer inclusion membranes, Water Res., 36 (2002) 4870–4876.

[14] V.K. Gupta, A.K. Shrivastava, N. Jain, Biosorption of chromium(VI) from aqueous solutions by green algae Spirogyra species, Water Res., 35 (2001) 4079–4085.

[15] H.F. Shaalan, M.H. Sorour, S.R. Tewfik, Simulation and optimization of a membrane system for chromium recovery from tanning wastes, Desalination, 141 (2001) 315–324.

[16] J.C. Seaman, P.M. Bertsch, L. Schwallie, *In-situ* Cr(VI) reduction within coarse-textured, oxide-coated soil and aquifer systems using Fe(II) solutions, Environ. Sci. Technol., 33 (1999) 938–944.

[17] S.K. Srivastava, V.K. Gupta, D. Mohan, Removal of lead and chromium by activated slag—a blast-furnace waste, J. Environ. Eng., 123 (1997) 461–468.

[18] D. Petruzzelli, R. Passino, G. Tiravanti, Ion exchange process for chromium removal and recovery from tannery wastes, Ind. Eng. Chem. Res., 34 (1995) 2612–2617.

[19] T.A. Saleh, Protocols for synthesis of nanomaterials, polymers, and green materials as adsorbents for water treatment technologies, Environ. Technol. Innovation, 24 (2021) 101821, doi: 10.1016/j.eti.2021.101821.

[20] T.A. Saleh, Nanomaterials: classification, properties, and environmental toxicities, Environ. Technol. Innovation, 20 (2020) 101067, doi: 10.1016/j.eti.2020.101067.

[21] T.A. Saleh, M. Mustaqeem, M. Khaled, Water treatment technologies in removing heavy metal ions from wastewater: a review, Environ. Nanotechnol. Monit. Manage., 17 (2022) 100617, doi: 10.1016/j.enmm.2021.100617.

[22] O.A. Bin-Dahman, T.A. Saleh, Synthesis of polyamide grafted on biosupport as polymeric adsorbents for the removal of dye and metal ions, Biomass Convers. Biorefin., (2022) 1–4, doi: 10.1007/s13399-022-02382-8.

[23] A. Alkenani, T.A. Saleh, Synthesis of amine-modified graphene integrated membrane as protocols for simultaneous rejection of hydrocarbons pollutants, metal ions, and salts from water, J. Mol. Liq., 367 (2022) 120291, doi: 10.1016/j.molliq.2022.120291.

[24] T.A. Saleh, Nanomaterials and hybrid nanocomposites for CO_2 capture and utilization: environmental and energy sustainability, RSC Adv., 12 (2022) 23869–23888.

[25] Z. Wang, C. Chen, H. Liu, D. Hrynshpan, T. Savitskaya, J. Chen, J. Chen, Enhanced denitrification performance of *Alcaligenes* sp. TB by Pd stimulating to produce membrane adaptation mechanism coupled with nanoscale zero-valent iron, Sci. Total Environ., 708 (2020) 135063, doi: 10.1016/j.scitotenv.2019.135063.

[26] M. Yang, H. Han, H. Jiang, S. Ye, X. Fan, J. Wu, Photoinduced reaction of potassium alkyltrifluoroborates, sulfur dioxide and *para*-quinone methides *via* radical 1,6-addition, Chin. Chem. Lett., 32 (2021) 3535–3538.

[27] Z. Song, D. Han, M. Yang, J. Huang, X. Shao, H. Li, Formic acid formation via direct hydration reaction ($CO + H_2O \rightarrow HCOOH$) on magnesia-silver composite, Appl. Surf. Sci., 607 (2023) 155067, doi: 10.1016/j.apsusc.2022.155067.

[28] K.L. Shih, J. Lederberg, Chloramine mutagenesis in *Bacillus subtilis*, Science, 192 (1976) 1141–1143.

[29] M. Ilyas, W. Ahmad, H. Khan, I. Ahmad, Application of composite adsorbents prepared from waste PS and PET for removal of Cr and Cu ions from wastewater, Desal. Water Treat., 171 (2019) 144–157.

[30] C.S. Umpierres, P.S. Thue, E.C. Lima, G.S. dos Reis, I.A.S. de Brum, W.S. de Alencar, S.L.P. Dias, G.L. Dotto, Microwave-activated carbons from tucumã (*Astrocaryum aculeatum*) seed for efficient removal of 2-nitrophenol from aqueous solutions, Environ. Technol., 39 (2018) 1173–1187.

[31] T.A. Saleh, Global trends in technologies and nanomaterials for removal of sulfur organic compounds: clean energy and green environment, J. Mol. Liq., 359 (2022) 119340, doi: 10.1016/j.molliq.2022.119340.

[32] T.A. Saleh, Advanced trends of shale inhibitors for enhanced properties of water-based drilling fluid, Upstream Oil Gas Technol., 8 (2022) 100069, doi: 10.1016/j.upstre.2022.100069.

[33] T.A. Saleh, Experimental and analytical methods for testing inhibitors and fluids in water-based drilling environments, TrAC, Trends Anal. Chem., 149 (2022) 116543, doi: 10.1016/j.trac.2022.116543.

[34] T.A. Saleh, G. Fadillah, E. Ciptawati, M. Khaled, Analytical methods for mercury speciation, detection, and measurement in water, oil, and gas, TrAC, Trends Anal. Chem., 132 (2020) 116016, doi: 10.1016/j.trac.2020.116016.

[35] Y. Dong, H. Yuan, H. Ge, N. Zhu, A novel conditioning approach for amelioration of sludge dewaterability using activated carbon strengthening electrochemical oxidation and realized mechanism, Water Res., 220 (2022) 118704.

[36] A.A. Alazab, T.A. Saleh, Magnetic hydrophobic cellulose-modified polyurethane filter for efficient oil-water separation in a complex water environment, J. Water Process Eng., 50 (2022) 103125, doi: 10.1016/j.jwpe.2022.103125.

[37] T.A. Saleh, Carbon nanotube-incorporated alumina as a support for MoNi catalysts for the efficient hydrodesulfurization of thiophenes, Chem. Eng. J., 404 (2021) 126987, doi: 10.1016/j.cej.2020.126987.

[38] A.M.D. Al Ketife, F. Almomani, H. Znad, Sustainable removal of copper from wastewater using chemically treated bio-sorbent: characterization, mechanism and process kinetics, Environ. Technol. Innovation, 23 (2021) 101555, doi: 10.1016/j.eti.2021.101555.

[39] E.N. Mahmoud, F.Y. Fayed, K.M. Ibrahim, S. Jaafreh, Removal of cadmium, copper, and lead from water using bio-sorbent from treated olive mill solid residue, Environ. Health Insights, 15 (2021), doi: 10.1177/11786302211053176.

[40] S. Sun, H. Liu, J. Zhang, W. Wang, P. Xu, X. Zhu, Y. Wang, S. Wan, Application of a novel coagulant in reservoir water treatment in Qingdao, Desal. Water Treat., 284 (2023) 49–60.

[41] X.H. Jiang, F. Yu, D.S. Wu, L. Tian, L.L. Zheng, L.S. Chen, P. Chen, L.S. Zhang, H. Zeng, Y. Chen, J.P. Zou, Isotypic heterojunction based on Fe-doped and terephthalaldehyde-modified carbon nitride for improving photocatalytic degradation with simultaneous hydrogen production, Chin. Chem. Lett., 32 (2021) 2782–2786.

[42] Y. Xu, C. Wu, Y. Wang, Y. Zhang, H. Sun, H. Chen, Y. Zhao, Cooperation between Pt and Ru on RuPt/AC bimetallic catalyst in the hydrogenation of phthalates, Chin. Chem. Lett., 32 (2021) 516–520.

[43] K.Z. Elwakeel, A.A. El-Bindary, E.Y. Kouta, E. Guibal, Functionalization of polyacrylonitrile/Na-Y-zeolite composite with amidoxime groups for the sorption of Cu(II), Cd(II) and Pb(II) metal ions, Chem. Eng. J., 332 (2018) 727–736.

[44] K. Rambabu, A. Thanigaivelan, G. Bharath, N. Sivarajasekar, F. Banat, P.L. Show, Biosorption potential of *Phoenix dactylifera* coir wastes for toxic hexavalent chromium sequestration, Chemosphere, 268 (2021) 128809, doi: 10.1016/j.chemosphere.2020.128809.

[45] K.Z. Elwakeel, A.S. Al-Bogami, A.M. Elgarahy, Efficient retention of chromate from industrial wastewater onto a green magnetic polymer based on shrimp peels, J. Polym. Environ., 26 (2018) 2018–2029.

[46] A. Mittal, R. Ahmad, I. Hasan, Biosorption of Pb^{2+}, Ni^{2+} and Cu^{2+} ions from aqueous solutions by L-cystein-modified montmorillonite-immobilized alginate nanocomposite, Desal. Water Treat., 57 (2016) 17790–17807.

[47] W.S. Chai, W.G. Tan, H.S.H. Munawaroh, V.K. Gupta, S.H. Ho, P.L. Show, Multifaceted roles of microalgae in the application of wastewater biotreatment: a review, Environ. Pollut., 269 (2021) 116236, doi: 10.1016/j.envpol.2020.116236.

[48] A.A. Atia, A.M. Donia, K.Z. ELwakeel, Adsorption behaviour of non-transition metal ions on a synthetic chelating resin bearing iminoacetate functions, Sep. Purif. Technol., 43 (2005) 43–48.

[49] A. Mittal, R. Ahmad, I. Hasan, Poly(methyl methacrylate)-grafted alginate/Fe_3O_4 nanocomposite: synthesis and its application for the removal of heavy metal ions, Desal. Water Treat., 57 (2016) 19820–19833.

[50] M. Agarwa, K. Singh, Heavy metal removal from wastewater using various adsorbents: a review, J. Water Reuse Desal., 7 (2017) 387–419.

[51] A.M. Elgarahy, K.Z. Elwakeel, S.H. Mohammad, G.A. Elshoubaky, A critical review of biosorption of dyes, heavy metals and metalloids from wastewater as an efficient and green process, Cleaner Eng. Technol., 4 (2021) 100209, doi: 10.1016/j.clet.2021.100209.

[52] N.M. Alandis, W. Mekhamer, O. Aldayel, J.A.A. Hefne, M. Alam, Adsorptive applications of montmorillonite clay for the removal of Ag(I) and Cu(II) from aqueous medium, J. Chem., 2019 (2019) 7129014, doi: 10.1155/2019/7129014.

[53] H. Zeng, L. Wang, D. Zhang, P. Yan, J. Nie, V.K. Sharma, C. Wang, Highly efficient and selective removal of mercury ions using hyperbranched polyethylenimine functionalized carboxymethyl chitosan composite adsorbent, Chem. Eng. J., 358 (2019) 253-263.

[54] A.M. Elgarahy, K.Z. Elwakeel, A. Akhdhar, M.F. Hamza, Recent advances in greenly synthesized nanoengineered materials for water/wastewater remediation: an overview, Nanotechnol. Environ. Eng., 6 (2021) 1–24.

[55] Z. Wang, L. Hu, M. Zhao, L. Dai, D. Hrynsphan, S. Tatsiana, J. Chen, Bamboo charcoal fused with polyurethane foam for efficiently removing organic solvents from wastewater: experimental and simulation, Biochar, 4 (2022) 28, doi: 10.1007/s42773-022-00153-2.

[56] Z. Wang, L. Dai, J. Yao, T. Guo, D. Hrynsphan, S. Tatsiana, J. Chen, Enhanced adsorption and reduction performance of nitrate by Fe–Pd–Fe$_3$O$_4$ embedded multi-walled carbon nanotubes, Chemosphere, 281 (2021) 130718, doi: 10.1016/j.chemosphere.2021.130718.

[57] Y. Liang, J. Li, Y. Xue, T. Tan, Z. Jiang, Y. He, W. Shangguan, J. Yang, Y. Pan, Benzene decomposition by non-thermal plasma: a detailed mechanism study by synchrotron radiation photoionization mass spectrometry and theoretical calculations, J. Hazard. Mater., 420 (2021) 126584, doi: 10.1016/j.jhazmat.2021.126584.

[58] C. Vanlalveni, S. Lallianrawna, A. Biswas, M. Selvaraj, B. Changmai, S.L. Rokhum, Green synthesis of silver nano-particles using plant extracts and their antimicrobial activities: a review of recent literature, RSC Adv., 11 (2021) 2804–2837.

[59] Md. R. Awual, Md. M. Hasan, A ligand based innovative composite material for selective lead(II) capturing from wastewater, J. Mol. Liq., 294 (2019) 111679, doi: 10.1016/j.molliq.2019.111679.

[60] K.Z. Elwakeel, A.M. Elgarahy, Z.A. Khan, M.S. Almughamisi, A.S. Al-Bogami, Perspectives regarding metal/mineral-incorporating materials for water purification: with special focus on Cr(VI) removal, Mater. Adv., 1 (2020) 1546–1574.

[61] A. Mittal, R. Ahmad, I. Hasan, Iron oxide-impregnated dextrin nanocomposite: synthesis and its application for the biosorption of Cr(VI) ions from aqueous solution, Desal. Water Treat., 57 (2016) 15133–15145.

[62] Md. R. Awual, Ring size dependent crown ether based mesoporous adsorbent for high cesium adsorption from wastewater, Chem. Eng. J., 303 (2016) 539–546.

[63] A. Benettayeb, A. Morsli, K.Z. Elwakeel, M.F. Hamza, E. Guibal, Recovery of heavy metal ions using magnetic glycine-modified chitosan—application to aqueous solutions and tailing leachate, Appl. Sci., 11 (2021) 8377, doi: 10.3390/app11188377.

[64] J. Mittal, R. Ahmad, A. Mariyam, V.K. Gupta, A. Mittal, Expeditious and enhanced sequestration of heavy metal ions from aqueous environment by papaya peel carbon: a green and low-cost adsorbent, Desal. Water Treat., 210 (2021) 365–376.

[65] Md. R. Awual, T. Yaita, S. Suzuki, H. Shiwaku, Ultimate selenium(IV) monitoring and removal from water using a new class of organic ligand based composite adsorbent, J. Hazard. Mater., 291 (2015) 111–119.

[66] K.Z. Elwakeel, A. Shahat, A.S. Al-Bogami, B. Wijesiri, A. Goonetilleke, The synergistic effect of ultrasound power and magnetite incorporation on the sorption/desorption behavior of Cr(VI) and As(V) oxoanions in an aqueous system, J. Colloid Interface Sci., 569 (2020) 76–88.

[67] C. Geng, F. Zhao, H. Niu, J. Zhang, H. Dong, Z. Li, H. Chen, Enhancing the permeability, anti-biofouling performance and long-term stability of TFC nanofiltration membrane by imidazole-modified carboxylated graphene oxide/polyethersulfone substrate, J. Membr. Sci., 664 (2022) 121099, doi: 10.1016/j.memsci.2022.121099.

[68] Y. Chen, C. Xu, W. Wang, X. Wang, Q. Guo, J. Shi, Phthalide-derived oxaspiroangelioic acids A–C with an unprecedented carbon skeleton from an aqueous extract of the *Angelica sinensis* root head, Chin. Chem. Lett., (2021) 3257–3260.

[69] J. Zhang, L. Wang, A. Zhong, G. Huang, F. Wu, D. Li, M. Teng, J. Wang, D. Han, Deep red PhOLED from dimeric salophen platinum(II) complexes, Dyes Pigm., 162 (2019) 590–598.

[70] R. Ahmad, I. Hasan, A. Mittal, Adsorption of Cr(VI) and Cd(II) on chitosan grafted polyaniline-OMMT nanocomposite: isotherms, kinetics and thermodynamics studies, Desal. Water Treat., 58 (2017) 144–153.

[71] Md. R. Awual, T. Yaita, T. Kobayashi, H. Shiwaku, S. Suzuki, Improving cesium removal to clean-up the contaminated water using modified conjugate material, J. Environ. Chem. Eng., 8 (2020) 103684, doi: 10.1016/j.jece.2020.103684.

[72] M.S. Almughamisi, Z.A. Khan, W. Alshitari, K.Z. Elwakeel, Recovery of chromium(VI) oxyanions from aqueous solution using Cu(OH)$_2$ and CuO embedded chitosan adsorbents, J. Polym. Environ., 28 (2020) 47–60.

[73] H. Daraei, A. Mittal, Investigation of adsorption performance of activated carbon prepared from waste tire for the removal of methylene blue dye from wastewater, Desal. Water Treat., 90 (2017) 294–298.

[74] Md. R. Awual, Assessing of lead(III) capturing from contaminated wastewater using ligand doped conjugate adsorbent, Chem. Eng. J., 289 (2016) 65–73.

[75] K.Z. Elwakeel, E. Guibal, Potential use of magnetic glycidyl methacrylate resin as a mercury sorbent: from basic study to the application to wastewater treatment, J. Environ. Chem. Eng., 4 (2016) 3632–3645.

[76] S. Soni, P.K. Bajpai, D. Bharti, J. Mittal, C. Arora, Removal of crystal violet from aqueous solution using iron-based metal organic framework, Desal. Water Treat., 205 (2020) 386–399.

[77] Z. Wang, X. Liu, S.Q. Ni, X. Zhuang, T. Lee, Nano zero-valent iron improves anammox activity by promoting the activity of quorum sensing system, Water Res., 202 (2021) 117491, doi: 10.1016/j.watres.2021.117491.

[78] S. Pang, C. Zhou, Y. Sun, K. Zhang, W. Ye, X. Zhao, L. Cai, B. Hui, Natural wood-derived charcoal embedded with bimetallic iron/cobalt sites to promote ciprofloxacin degradation, J. Cleaner Prod., 414 (2023) 137569, doi: 10.1016/j.jclepro.2023.137569.

[79] H.C. Wang, Y. Liu, Y.M. Yang, Y.K. Fang, S. Luo, H.Y. Cheng, A.J. Wang, Element sulfur-based autotrophic denitrification constructed wetland as an efficient approach for nitrogen removal from low C/N wastewater, Water Res., 226 (2022) 119258, doi: 10.1016/j.watres.2022.119258.

[80] Md. R. Awual, T. Yaita, H. Shiwaku, Design a novel optical adsorbent for simultaneous ultra-trace cerium(III) detection, sorption and recovery, Chem. Eng. J., 228 (2013) 327–335.

[81] Md. R. Awual, Solid phase sensitive palladium(II) ions detection and recovery using ligand based efficient conjugate nanomaterials, Chem. Eng. J., 300 (2016) 264–272.

[82] Md. R. Awual, A novel facial composite adsorbent for enhanced copper(II) detection and removal from wastewater, Chem. Eng. J., 266 (2015) 368–375.

[83] Md. R. Awual, A facile composite material for enhanced cadmium(II) ion capturing from wastewater, J. Environ. Chem. Eng., 7 (2019) 103378, doi: 10.1016/j.jece.2019.103378.

[84] D. Khedri, A.H. Hassani, E. Moniri, H.A. Panahi, M. Khaleghian, Efficient removal of phenolic contaminants from wastewater samples using functionalized graphene oxide with thermo-sensitive polymer: adsorption isotherms, kinetics, and thermodynamics studies, Surf. Interfaces, 35 (2022) 102439, doi: 10.1016/j.surfin.2022.102439.

[85] E. Hesabi, M. Nikpour Nezhati, H. Ahmad Panahi, F. Bandarchian, E. Moniri, Synthesis of MoS$_2$/Fe$_3$O$_4$/aminosilane/glycidyl methacrylate/melamine grafted polystyrene/poly(N-vinylcaprolactam) nanocomposite for adsorption and controlled release of sertraline from aqueous solutions, Int. J. Polym. Mater. Polym. Biomater., 71 (2022) 1090–1103.

[86] A. Hajighasemkhan, L. Taghavi, E. Moniri, A.H. Hassani, H.A. Panahi, Adsorption kinetics and isotherms study of 2,4-dichlorophenoxyacetic acid by 3dimensional/graphene oxide/magnetic from aquatic solutions, Int. J. Environ. Anal. Chem., 102 (2022) 1171–1191.

[87] A. Azizi, E. Moniri, A.H. Hassani, H.A. Panahi, M. Jafarinezhad, Nonlinear and linear analysis of Direct Yellow 50 adsorption onto modified graphene oxide: kinetic, isotherm, and thermodynamic studies, Desal. Water Treat., 229 (2021) 352–361.

[88] M. Ilyas, W. Ahmad, H. Khan, Polycyclic aromatic hydrocarbons removal from vehicle-wash wastewater using activated char, Desal. Water Treat., 236 (2021) 55–68.

[89] M. Ilyas, H. Khan, W. Ahmad, Conversion of waste plastics into carbonaceous adsorbents and their application for wastewater treatment, Int. J. Environ. Anal. Chem., (2022) 1–9, doi: 10.1080/03067319.2022.2062571.

[90] S.C. Tsai, K.W. Juang, Comparison of linear and non-linear forms of isotherm models for strontium sorption on a sodium bentonite, J. Radioanal. Nucl. Chem., 243 (2000) 741–746.

[91] W. Liu, C. Zhao, Y. Zhou, X. Xu, Modeling of vapor-liquid equilibrium for electrolyte solutions based on COSMO-RS interaction, J. Chem., 29 (2022) 1–3.

[92] X. Zhang, F. Ma, Z. Dai, J. Wang, L. Chen, H. Ling, M.R. Soltanian, Radionuclide transport in multi-scale fractured rocks: a review, J. Hazard. Mater., 424 (2022) 127550, doi: 10.1016/j.jhazmat.2021.127550.

[93] D. Chen, Q. Wang, Y. Li, Y. Li, H. Zhou, Y. Fan, A general linear free energy relationship for predicting partition coefficients of neutral organic compounds, Chemosphere, 247 (2020) 125869, doi: 10.1016/j.chemosphere.2020.125869.

[94] M. Ilyas, W. Ahmad, H. Khan, Utilization of activated carbon derived from waste plastic for decontamination of polycyclic aromatic hydrocarbons laden wastewater, Water Sci. Technol., 84 (2021) 609–631.

[95] W. Liu, J. Zheng, X. Ou, X. Liu, Y. Song, C. Tian, W. Rong, Z. Shi, Z. Dang, Z. Lin, Effective extraction of Cr(VI) from hazardous gypsum sludge via controlling the phase transformation and chromium species, Environ. Sci. Technol., 52 (2018) 13336–13342.

[96] G. Xia, Y. Zheng, Z. Sun, S. Xia, Z. Ni, J. Yao, Fabrication of ZnAl-LDH mixed metal-oxide composites for photocatalytic degradation of 4-chlorophenol, Environ. Sci. Pollut. Res., 29 (2022) 39441–39450.

[97] X. Zhang, Z. Wang, P. Reimus, F. Ma, M.R. Soltanian, B. Xing, J. Zang, Y. Wang, Z. Dai, Plutonium reactive transport in fractured granite: multi-species experiments and simulations, Water Res., 224 (2022) 119068, doi: 10.1016/j.watres.2022.119068.

[98] C.P. Dwivedi, J.N. Sahu, C.R. Mohanty, B.R. Mohan, B.C. Meikap, Column performance of granular activated carbon packed bed for Pb(II) removal, J. Hazard. Mater., 156 (2008) 596–603.

[99] J. Yuan, T.J. Wang, J. Chen, Microscopic mechanism study of the creep properties of soil based on the energy scale method, Front. Mater., 10 (2023) 1137728, doi: 10.3389/fmats.2023.1137728.

[100] Z. Aly, A. Graulet, N. Scales, T. Hanley, Removal of aluminium from aqueous solutions using PAN-based adsorbents: characterisation, kinetics, equilibrium and thermodynamic studies, Environ. Sci. Pollut. Res., 21 (2014) 3972–3986.

[101] S.A. Al-Muhtaseb, M.H. El-Naas, S. Abdallah, Removal of aluminum from aqueous solutions by adsorption on date-pit and BDH activated carbons, J. Hazard. Mater., 158 (2008) 300–307.

[102] A. Islam, H. Ahmad, N. Zaidi, S. Yadav, Selective separation of aluminum from biological and environmental samples using glyoxal-bis(2-hydroxyanil) functionalized Amberlite XAD-16 resin: kinetics and equilibrium studies, Ind. Eng. Chem. Res., 52 (2013) 5213–5220.

[103] M. Luo, S. Bi, Solid phase extraction–spectrophotometric determination of dissolved aluminum in soil extracts and ground waters, J. Inorg. Biochem., 97 (2003) 173–178.

[104] J.L. Boudenne, S. Boussetta, C. Brach-Papa, C. Branger, A. Margaillan, F. Théraulaz, Modification of poly(styrene-co-divinylbenzene) resin by grafting on an aluminium selective ligand, Polym. Int., 51 (2002) 1050–1057.

[105] F. An, B. Gao, X. Huang, Y. Zhang, Y. Li, Y. Xu, Z. Zhang, J. Gao, Z. Chen, Selectively removal of Al(III) from Pr(III) and Nd(III) rare earth solution using surface imprinted polymer, React. Funct. Polym., 73 (2013) 60–65.